

## Chapter 6

# Superplasticity

### 6.1 INTRODUCTION

Superplasticity is the ability of a polycrystalline material to exhibit, in a generally isotropic manner, very high tensile elongations prior to failure ( $T > 0.5 T_m$ ) [406]. The first observations of this phenomenon were made as early as 1912 [407]. Since then, Superplasticity has been extensively studied in metals. It is believed that both the arsenic bronzes, used in Turkey in the Bronze Age (2500 B.C.), and the Damascus steels, utilized from 300 B.C. to the end of the nineteenth century, were already superplastic materials [408]. One of the most spectacular observations of Superplasticity is perhaps that reported by Pearson in 1934 of a Bi-Sn alloy that underwent nearly 2000% elongation [409]. He also claimed then, for the first time, that grain-boundary sliding was the main deformation mechanism responsible for superplastic deformation. The interest in Superplasticity has increased due to the recent observations of this phenomenon in a wide range of materials, including some materials (such as nanocrystalline materials [410], ceramics [411,412], metal matrix composites [413], and intermetallics [414]) that are difficult to form by conventional forming. Recent extensive reviews on Superplasticity are available [415–418].

There are two types of superplastic behavior. The best known and studied, fine-structure Superplasticity (FSS), will be briefly discussed in the following sections. The second type, Internal stress Superplasticity (ISS), refers to the development of Internal stresses in certain materials, which then deform to large tensile strains under relatively low externally applied stresses [418].

### 6.2 CHARACTERISTICS OF FINE STRUCTURE SUPERPLASTICITY

Fine structure superplastic materials generally exhibit a high strain-rate sensitivity exponent ( $m$ ) during tensile deformation. Typically,  $m$  is larger than 0.33. Thus,  $n$  in equation (3), is usually smaller than 3. In particular, the highest elongations have been reported to occur when  $m \sim 0.5$  ( $n \sim 2$ ) [418]. Superplasticity in conventional materials usually occurs at low strain rates ranging from  $10^{-3} \text{ s}^{-1}$  to  $10^{-5} \text{ s}^{-1}$ . However, it has been reported in recent works that large elongations to failure may also occur in selected materials at strain rates substantially higher than  $10^{-2} \text{ s}^{-1}$  [419]. This phenomenon, termed high-strain-rate Superplasticity (HSRSP), has been observed in some conventional metallic alloys, in metal matrix composites and in

mechanically alloyed materials [420], among others. This will be discussed in Section 6.5. Very recently, HSRSP has been observed in cast alloys prepared by ECA (equal channel angular) extrusion [421–424]. In this case, very high temperatures are not required and the grain size is very small ( $< 1 \mu\text{m}$ ). The activation energies for fine structure superplasticity tend to be low, close to the value for grain boundary diffusion, at intermediate temperatures. At high temperatures, however, the activation energy for superplastic flow is about equal to that for lattice diffusion.

The microscopic mechanism responsible for superplastic deformation is still not thoroughly understood. However, since Pearson's first observations [409], the most widely accepted mechanisms involve grain-boundary sliding (GBS) [425–432]. GBS is generally modeled assuming sliding takes place by the movement of extrinsic dislocations along the grain boundary. This would account for the observation that the amount of sliding is variable from point to point along the grain boundary [433]. Dislocation pile-ups at grain boundary ledges or triple points may lead to stress concentrations. In order to avoid extensive cavity growth, GBS must be aided by an accommodation mechanism [434]. The latter must ensure rearrangement of grains during deformation in order to achieve strain compatibility and relieve any stress concentrations resulting from GBS. The accommodation mechanism may include grain boundary migration, recrystallization, diffusional flow or slip. The accommodation process is generally believed to be the rate-controlling mechanism.

Over the years a large number of models have emerged in which the accommodation process is either diffusional flow or dislocation movement [435]. The best known model for GBS accommodated by diffusional flow, depicted schematically in Figure 58, was proposed by Ashby and Verral [436]. This model

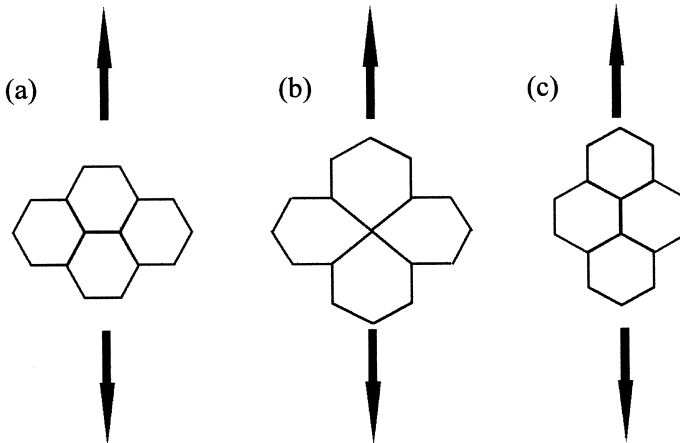


**Figure 58.** Ashby–Verral model of GBS accommodated by diffusional flow [436].

explains the experimentally observed switching of equiaxed grains throughout deformation. However, it fails to predict the stress dependence of the strain-rate. According to this model,

$$\dot{\epsilon}_{ss} = K_1(b/g)^2 D_{\text{eff}}(\sigma - \sigma_{TH_s}/E) \quad (99)$$

where  $D_{\text{eff}} = D_{\text{sd}} \cdot 9 [1 + (3.3 w/g)(D_{\text{gb}}/D_{\text{sd}})]$ ,  $K_1$  is a constant,  $\sigma_{TH_s}$  is the threshold stress and  $w$  is the grain boundary width. The threshold stress arises since there is an increase in boundary area during grain switching when clusters of grains move from the initial position (Figure 58(a)) to the intermediate one (Figure 58(b)).

Several criticisms of this model have been reported [437–442]. According to Spingarn and Nix [437] the grain rearrangement proposed by Ashby–Verral cannot occur purely by diffusional flow. The diffusion paths are physically incorrect. The first models of GBS accommodated by diffusional creep were proposed by Ball and Hutchison [443], Langdon [444], and Mukherjee [445]. Among the most cited are those proposed by Mukherjee and Arieli [446] and Langdon [447]. According to these authors, GBS involves the movement of dislocations along the grain boundaries, and the stress concentration at triple points is relieved by the generation and movement of dislocations within the grains (Figure 59). Figure 60 illustrates the model proposed by Gifkins [448], in which the accommodation process, which also consists of dislocation movement, only occurs in the “mantle” region of the grains, i.e., in the region close to the grain boundary. According to all these GBS accommodated by slip models,  $n = 2$  in a relationship such as

$$\dot{\epsilon}_{ss} = K_2(b/g)^p D(\sigma/E)^2 \quad (100)$$

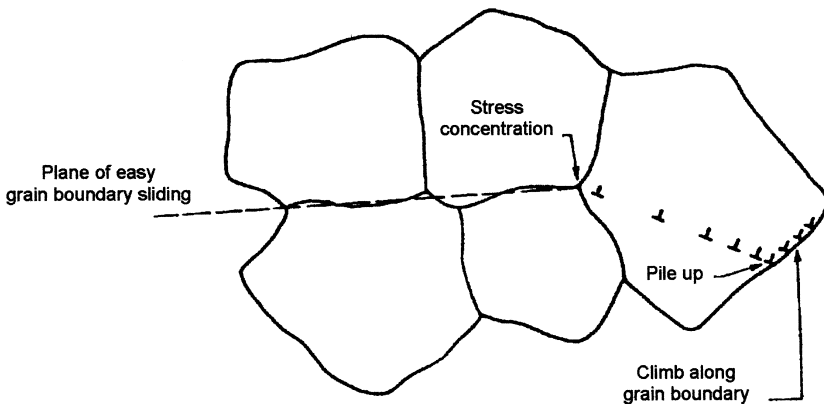


Figure 59. Ball–Hutchinson model of GBS accommodated by dislocation movement [443].

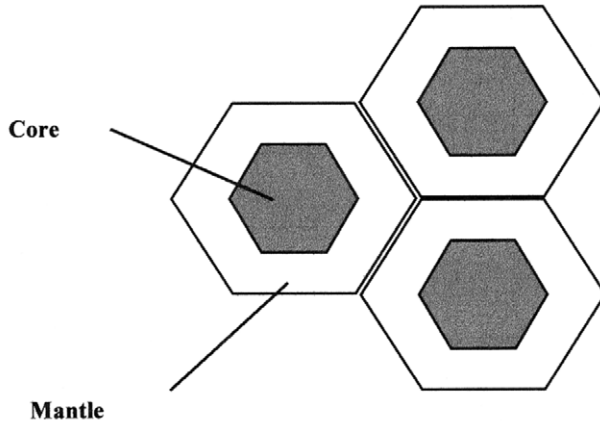


Figure 60. Gifkins “core and mantle” model [448].

where  $p' = 2$  or  $3$  depending on whether the dislocations move within the lattice or along the grain boundaries, respectively.  $K_2$  is a constant, which varies with each of the models and the diffusion coefficient,  $D$ , can be  $D_{sd}$  or  $D_{gb}$ , depending on whether the dislocations move within the lattice or along the grain boundaries to accommodate stress concentrations from GBS. In order to rationalize the increase in activation energy at high temperatures, Fukuyo *et al.* [449] proposed a model based on the GBS mechanism in which the dislocation accommodation process takes place by sequential steps of climb and glide. At intermediate temperatures, climb along the grain boundaries is the rate-controlling mechanism due to the pile-up stresses. Pile-up stresses are absent and the glide of dislocations within the grain is the rate-controlling mechanism at high temperatures. It is believed that slip in Superplasticity is accommodating and does not contribute to the total strain [450]. Thus, GBS is traditionally believed to account for all of the strain in Superplasticity [451]. However, recent studies, based on texture analysis, indicate that slip may contribute to the total elongation [452–467].

The proposed mechanisms predict some behavior but have not succeeded in fully predicting the dependence of the strain rate on  $\sigma$ ,  $T$ , and  $g$  during superplastic deformation. Ruano and Sherby [468,469] formulated the following phenomenological equations, which appear to describe the experimental data from metallic materials,

$$\dot{\epsilon}_{ss} = K_3(b/g)^2 D_{sd}(\sigma/E)^2 \quad (101)$$

$$\dot{\epsilon}_{ss} = K_4(b/g)^3 D_{gb}(\sigma/E)^2 \quad (102)$$

where  $K_3$  and  $K_4$  are constants. These equations, with  $n=2$ , correspond to a mechanism of GBS accommodated by dislocation movement. Equation (101) corresponds to an accommodation mechanism in which the dislocations would move within the grains ( $g^2$ ) and equation (102) corresponds to an accommodation mechanism in which the dislocations would move along the grain boundaries ( $g^3$ ). Only the sliding of individual grains has been considered. However, currently the concept of cooperative grain-boundary sliding (CGBS), i.e., the sliding of blocks of grains, is gaining increasing acceptance. Several deformation models that account for CGBS are described in Ref. [421].

### 6.3 MICROSTRUCTURE OF FINE STRUCTURE SUPERPLASTIC MATERIALS

The microstructures associated with fine structure superplasticity are well established for conventional metallic materials. They are, however, less clearly defined for intermetallics, ceramics, metal matrix composites, and nanocrystalline materials.

#### 6.3.1 Grain Size and Shape

GBS in metals is favored by the presence of equiaxed small grains that should generally be smaller than  $10\ \mu\text{m}$ . Consistent with equations (99–102), the strain-rate is usually inversely proportional to grain size, according to

$$\dot{\epsilon}_{ss} = K_5 g^{-p'} \quad (103)$$

where  $p' = 2$  or  $3$  depending, perhaps, on the accommodation mechanism and  $K_5$  is a constant. Also, for a given strain-rate, the stress decreases as grain size decreases. grain size refinement is achieved during the thermomechanical processing by successive stages of warm and cold rolling [468–473]. However, the present understanding of microstructural control in engineering alloys during industrial processing by deformation and recrystallization is still largely empirical.

#### 6.3.2 Presence of a Second Phase

The presence of small second-phase particles uniformly distributed in the matrix prevents rapid grain growth that can occur in single-phase materials within the temperature range over which Superplasticity is observed.

#### 6.3.3 Nature and Properties of Grain Boundaries

GBS is favored along high-angle disordered (not CSL) boundaries. Additionally, sliding is influenced by the grain boundary composition. For example, a heterophase

boundary (i.e., a boundary which separates grains with different chemical composition) slides more readily than a homophase boundary. Stress concentrations develop at triple points and at other obstacles along the grain boundaries as a consequence of GBS. mobile grain boundaries may assist in relieving these stresses. Grain boundaries in the matrix phase should not be prone to tensile separation.

#### **6.4 TEXTURE STUDIES IN SUPERPLASTICITY**

texture analysis has been utilized to further study the mechanisms of Superplasticity [442–467,474], using both X-ray texture analysis and computer-aided EBSD techniques [475]. Commonly, GBS, involving grain rotation, is associated with a decrease in texture [417], whereas crystallographic slip leads to the stabilization of certain preferred orientations, depending on the number of slip systems that are operating [476,477].

It is interesting to note that a large number of investigations based on texture analysis have led to the conclusion that crystallographic slip (CS) is important in superplastic deformation. According to these studies, CS is not merely an accommodation mechanism for GBS, but also operates in direct response to the applied stress. Some investigators [453–458,474] affirm that both GBS and CS coexist at all stages of deformation; other investigators [459–461] conclude that CS only operates during the early stages of deformation, leading to a microstructure favoring GBS. Others [462–467] even suggest that CS is the principal deformation mechanism responsible for superplastic deformation.

#### **6.5 HIGH STRAIN-RATE SUPERPLASTICITY**

High strain-rate Superplasticity (HSRS) has been defined by the Japanese Standards Association as Superplasticity at strain-rates equal to or greater than  $10^{-2} \text{ s}^{-1}$  [418,478,479]. This field has awakened considerable interest in the last 15 years since these high strain-rates are close to the ones used for commercial applications ( $10^{-2} \text{ s}^{-1}$  to  $10^{-1} \text{ s}^{-1}$ ). Higher strain-rates can be achieved by reducing the grain size [see equation (100)] or by engineering the nature of the interfaces in order to make them more suitable for sliding [478,479]. High strain-rate Superplasticity was first observed in a 20%SiC whisker reinforced 2124 Al composite [419]. Since then, it has been achieved in several metal–matrix composites, mechanically alloyed materials, conventional alloys that undergo Continuous reactions or (continuous dynamic recrystallization), alloys processed by power consolidation, by physical vapor deposition, by intense plastic straining [480] (for example, equal channel angular

pressing (ECAP), equal channel angular extrusion (ECAE), torsion straining under high pressure), or, more recently, by friction stir processing [481]. The details of the microscopic mechanism responsible for high strain-rate Superplasticity are not yet well understood, but some recent theories are reviewed below.

### 6.5.1 High Strain-Rate Superplasticity in Metal–Matrix Composites

High strain-rate Superplasticity has been achieved in a large number of metal–matrix composites. Some of them are listed in Table 2 and more complete lists can be found elsewhere [478,482]. The microscopic mechanism responsible for high strain-rate Superplasticity in metal–matrix composites is still a matter of controversy. Any theory must account for several common features of the mechanical behavior of metal–matrix composites that undergo high strain-rate Superplasticity, such as [491]:

- (a) Maximum elongations are achieved at very high temperatures, sometimes even slightly higher than the incipient melting point.
- (b) The strain-rate sensitivity exponent changes at such high temperatures from  $\sim 0.1$  ( $n \sim 10$ ) (low strain-rates) to  $\sim 0.3$  ( $n \sim 3$ ) (high strain-rates).
- (c) High apparent activation energy values are observed. Values of 920 kJ/mol and 218 kJ/mol have been calculated for  $\text{SiC}_w/2124\text{Al}$  at low and high strain-rates, respectively. These values are significantly higher than the activation energy for self-diffusion in Al (140 kJ/mol).

Both grain-boundary sliding and interfacial sliding have been proposed as the mechanisms responsible for HSRS. The significant contribution of interfacial sliding is evidenced by extensive fiber pullout apparent on fracture surfaces [491]. However, an accommodation mechanism has to operate simultaneously in order to avoid

**Table 2.** Superplastic characteristics of some metal–matrix composites exhibiting high strain-rate superplasticity.

| Material                                 | Temperature ( $^{\circ}\text{C}$ ) | Strain rate ( $\text{s}^{-1}$ ) | Elongation (%) | Reference |
|--|------------------------------------|---------------------------------|----------------|-----------|
| $\text{SiC}_w/2124\text{Al}$             | 525                                | 0.3                             | $\sim 300$     | [419]     |
| $\text{SiC}_w/2024\text{Al}$             | 450                                | 1                               | 150            | [483]     |
| $\text{SiC}_w/6061\text{Al}$             | 550                                | 0.2                             | 300            | [484]     |
| $\text{SiC}_p/7075\text{Al}$             | 520                                | 5                               | 300            | [485]     |
| $\text{SiC}_p/6061\text{Al}$             | 580                                | 0.1                             | 350            | [486]     |
| $\text{Si}_3\text{N}_{4w}/6061\text{Al}$ | 545                                | 0.5                             | 450            | [487]     |
| $\text{Si}_3\text{N}_{4w}/2124\text{Al}$ | 525                                | 0.2                             | 250            | [488]     |
| $\text{Si}_3\text{N}_{4w}/5052\text{Al}$ | 545                                | 1                               | 700            | [489]     |
| $\text{AlN}/6061\text{Al}$               | 600                                | 0.5                             | 350            | [490]     |

(w = whisker; p = particle).

cavitation at such high strain-rates. The nature of this accommodation mechanism, that enables the boundary and interface mobility, is still uncertain.

A fine matrix grain size is necessary but not sufficient to explain high strain-rate Superplasticity. In fact, HSRS may or may not appear in two composites having the same fine-grained matrix and different reinforcements. For example, it has been found that a 6061 Al matrix with  $\beta$ -Si<sub>3</sub>N<sub>4</sub> whiskers does experience HSRS, whereas the same matrix with  $\beta$ -SiC does not [491]. The nature, size, and distribution of the reinforcement are critical to the onset of high strain-rate Superplasticity.

**a. Accommodation by a Liquid Phase. Rheological Model.** Nieh and Wadsworth [491] have proposed that the presence of a liquid phase at the matrix-reinforcement interface and at grain boundaries within the matrix is responsible for accommodation of interface sliding during HSRS and thus for strain-rate enhancement. The presence of this liquid phase would be responsible for the observed high activation energies. A small grain size would favor HSRS since the liquid phase would then be distributed along a larger surface area and thus can have a higher capillarity effect, preventing decohesion. The occurrence of partial melting even during tests at temperatures slightly below solvus has been explained in two different ways. First, as a consequence of solute segregation, a low melting point region could be created at the matrix-reinforcement interfaces. Alternatively, local adiabatic heating at the high strain-rates used could contribute to a temperature rise that may lead to local melting.

It has been suggested [492] that high strain-rate Superplasticity with the aid of a liquid phase can be modeled in rheological terms in a similar way to semi-solid metal forming. A fluid containing a suspension of particles behaves like a non-Newtonian fluid, for which the strain-rate sensitivity and the shear strain-rate are related by

$$\tau = K_7 \cdot \dot{\gamma}^m \quad (104)$$

where  $\tau$  is the shear stress, and  $K_7$  and  $m$  are both materials constants,  $m$  being the strain-rate sensitivity of the material. The shear stress and strain rate of a semi-solid that behaves like a non-Newtonian fluid are related to the shear viscosity by the following equations:

$$\eta = K_7 \cdot \dot{\gamma}^{-u} \quad (105)$$

$$\eta = \tau / \dot{\gamma} \quad (106)$$

where  $\eta$  is the shear viscosity and  $u$  is a constant of the material, related to the strain-rate sensitivity by the expression  $m = 1 - u$ . The viscosity of several Al-6.5%Si metal matrix composites was measured experimentally [418] at 700°C as a function of shear rate. High strain sensitivity values similar to those reported for MMCs ( $\sim 0.3$ – $0.5$ ) in



the HSRS regime were obtained at very high shear strain rates (200–1000 s<sup>-1</sup>). These data support the rheological model. The temperature used, however, is higher than the temperatures at which high strain-rate Superplasticity is observed.

The role of a liquid phase as an accommodation mechanism for interfacial and grain-boundary sliding has been supported by other authors [493–498]. It is suggested that the liquid phase acts as an accommodation mechanism, relieving stresses originated by sliding and thus preventing cavity formation. However, in order to avoid decohesion, it is emphasized that the liquid phase must either be distributed discontinuously or be present in the form of a thin layer. The optimum amount of liquid phase may depend on the nature of the grain boundary or interface. Direct evidence of local melting at the reinforcement–matrix interface was obtained using *In situ* transmission electron microscopy by Koike *et al.* [495] in a Si<sub>3</sub>N<sub>4p</sub>/6061 Al. The rheological model was criticized by Mabuchi *et al.* [493], arguing that testing the material at a temperature within the solid–liquid region is not sufficient to achieve high strain-rate Superplasticity. For example, an unreinforced 2124 alloy fails to exhibit high tensile ductility when tested at a temperature above solvus. Additionally, it has been observed experimentally that ductility decreases when testing above a certain temperature.

**b. Accommodation by Interfacial Diffusion.** Mishra *et al.* [499–502] rationalized the mechanical behavior of HSRS metal–matrix composites by taking into account the presence of a threshold stress. This analysis led them to conclude that the mechanism responsible for HSRS in metal–matrix composites is grain-boundary sliding accommodated by interfacial diffusion along matrix–reinforcement interfaces. It is important to note that the particle size is often comparable to grain size, and therefore interfacial sliding is geometrically necessary, as illustrated in Figure 61. Partial melting, especially if it is confined to triple points, may be beneficial for superplastic deformation, but it is not necessary to account for the superplastic elongations observed.

Threshold stresses are often used to explain the variation of the strain-rate sensitivity exponent with strain-rate in creep deformation studies. The presence of a threshold stress would explain the transition to a lower strain-rate sensitivity value (and, thus, to a higher  $n$ ) at low strain rates that takes place during HSRS in metal–matrix composites. Calculating threshold stresses and a (true) stress exponent,  $n_{\text{HSRS}}$ , that describes the predominant deformation mechanism is a non-trivial process, as explained in Ref. [500]. Mishra *et al.* [500,501] concluded that a true stress exponent of 2 would give the best fit for their data, suggesting the predominance of grain-boundary sliding as a deformation mechanism responsible for HSRS in metal–matrix composites. Additionally, activation energies ( $Q_{\text{HSRS}}$ ) of the order of

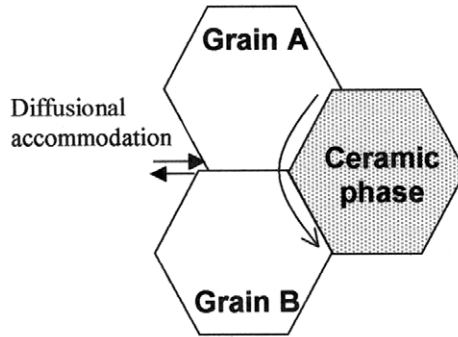


**Figure 61.** Interfacial diffusion-controlled grain-boundary sliding. The ceramic phase would not allow slip accommodation.

300 kJ/mol were obtained from this analysis. Both parametric dependencies ( $n_{\text{hsrs}} = 2$  and  $Q_{\text{hsrs}} \cong 300$  kJ/mol) are best predicted by Arzt's model for "interfacial diffusion-controlled diffusional creep" [503]. Mishra *et al.* [502] suggested that, since both diffusional creep and grain-boundary sliding are induced by the movement of grain-boundary dislocations, and the atomic processes involved are similar for both processes, it is reasonable to think that the parametric dependencies would be similar in both interfacial diffusion-controlled diffusional creep and interfacial diffusion-controlled Superplasticity. Thus, the latter is invoked to be responsible for HSRS. Figure 61 illustrates this deformation mechanism.

The phenomenological constitutive equation proposed by Mishra *et al.* for HSRS in metal–matrix composites is the following:

$$\dot{\epsilon}_{\text{ss}} = A_{12} \frac{D_i G b}{kT} \left( \frac{b^2}{g_m g_p} \right) \left( \frac{\sigma - \sigma_{\text{TH}_{\text{hsrs}}}}{E} \right)^2 \quad (107)$$

where  $D_i$  is the coefficient for interfacial diffusion,  $g_m$  is the matrix grain size and  $g_p$  is the particle/reinforcement size,  $\sigma_{\text{TH}_{\text{hsrs}}}$  is the threshold stress for high strain-rate Superplasticity, and  $A_{12}$  is a material constant. An inverse grain size and reinforcement size dependence is suggested.

According to this model [501], as temperature rises, the accommodation mechanism would change from slip accommodation (at temperatures lower than the optimum) to interfacial diffusion accommodation. The need for very high temperatures to attain HSRS is due to the fact that grain-boundary diffusivity increases with temperature. Therefore, the higher the temperature, the faster interface diffusion, which leads to less cavitation and thus, higher ductility.

Mabuchi *et al.* [504,505] claim the importance of a liquid phase in HSRS arguing that, when introducing threshold stresses, the activation energy for HSRS at

temperatures at which no liquid phase is present is similar to that corresponding to lattice self-diffusion in Al. However, at higher temperatures, at which partial melting has taken place, the activation energy increases dramatically. It is at these temperatures that the highest elongations are observed. The origin of the threshold stress for Superplasticity is not well known. Its magnitude depends on the shape and size of the reinforcement and it generally decreases with increasing temperature.

**c. Accommodation by Grain-Boundary Diffusion in the Matrix. The Role of Load Transfer.** The two theories described above were critically examined by Li and Langdon [506–508]. First, the rheological model was questioned, since HSRS had been recently found in Mg–Zn metal–matrix composites at temperatures below the incipient melting point, where no liquid phase is present [509]. Second, Li *et al.* [506] claim that it is hard to estimate interfacial diffusion coefficients at ceramic–matrix interfaces, and therefore validation of the interfacial diffusion-controlled grain-boundary sliding mechanism is difficult. These investigators used an alternative method for computing threshold stresses, described in detail in Ref. [506], which does not require an initial assumption of the value of  $n$ . This methodology also rendered a true stress exponent of 2 and true activation energy values that were higher than that for matrix lattice self-diffusion and grain boundary self-diffusion. These results were explained by the occurrence of a transfer of load from the matrix to the reinforcement. Following this approach, that was used before to rationalize creep behavior in metal–matrix composites [510], a temperature-dependent load-transfer coefficient  $\alpha'$  was incorporated in the constitutive equation as follows:

$$\dot{\epsilon}_{ss} = \frac{A'''' DGb}{kT} \left(\frac{b}{g}\right)^{p'} \left[ \frac{(1-\alpha')(\sigma - \sigma_{TH_{HSRS}})}{G} \right]^n \quad (108)$$

where  $A''''$  is a dimensionless constant. In their calculations, Li *et al.* assumed that  $D$  is equal to  $D_{gb}$  and the remaining constants and variables have the usual meaning. Load-transfer coefficients are expected to vary between 0 (no load-transfer) and 1 (all the load is transferred to the reinforcement). It was found that the load-transfer coefficients obtained decreased with increasing temperature, becoming 0 at temperatures very close to the incipient melting point. This indicates that load transfer would be inefficient in the presence of a liquid phase. The effective activation energies  $Q^*$  calculated by introducing the load-transfer coefficient into the rate equation for flow are similar to those corresponding to grain-boundary diffusion within the matrix alloys (until up to a few degrees from the incipient melting point). Therefore, Li and Langdon proposed that the mechanism responsible for HSRS is grain-boundary sliding controlled by grain-boundary diffusion in the matrix. This mechanism, that

is characteristic of conventional Superplasticity at high temperatures, would be valid up to temperatures close to the incipient melting point.

The origin of the threshold stress is still uncertain. It has been shown that it decreases with increasing temperature, and that it depends on the shape and size of the reinforcement [502]. The temperature dependence of the threshold stress may be expressed by an Arrhenius-type equation of the form:

$$\frac{\sigma_{\text{TH}_{\text{hsrs}}}}{G} = B \exp\left(\frac{Q_{\text{TH}_{\text{hsrs}}}}{RT}\right) \quad (109)$$

where  $\sigma_{\text{TH}_{\text{hsrs}}}$  is the threshold stress for high strain-rate Superplasticity,  $B$  is a constant, and  $Q_{\text{TH}_{\text{hsrs}}}$  is an energy term which seems to be associated with the process by which the mobile dislocations surpass the obstacles in the glide planes. (The threshold stress concept will be discussed again in Chapter 8.)

Li and Langdon [508] claim that the threshold stress values obtained in metal–matrix composites tested under HSRS and under creep conditions may have the same origin. They showed that similar values of  $Q_{\text{TH}_{\text{hsrs}}}$  are obtained under these two conditions when, in addition to load transfer, substructure strengthening is introduced into the rate equation for flow. Substructure strengthening may arise, for example, from an increase in the dislocation density due to the thermal mismatch between the matrix and the reinforcement or to the resistance of the reinforcement to plastic flow. The “effective stress” acting on the composite in the presence of load-transfer and substructure strengthening is given by,

$$\sigma_e = (1 - \Phi)\sigma - \sigma_{\text{TH}_{\text{hsrs}}} \quad (110)$$

where  $\Phi$  is a temperature-dependent coefficient. At low temperatures at which creep tests are performed, the value of  $\Phi$  may be negligible, but since HSRS takes place at very high temperatures, often close to the melting point, the temperature dependence of  $\Phi$  must be taken into account to obtain accurate values of  $Q_{\text{TH}_{\text{hsrs}}}$ . In fact, when the temperature dependence of  $\Phi$  is considered,  $Q_{\text{TH}_{\text{hsrs}}}$  values close to 20–30 kJ/mol, typical of creep deformation of MMCs, are obtained under HSRS conditions.

### 6.5.2 High Strain-Rate Superplasticity in Mechanically Alloyed Materials

HSRS has also been observed in some mechanically alloyed (MA) materials that are listed in Table 3.

As can be observed in Table 3, mechanically alloyed materials attain superplastic elongations at higher strain-rates than metal–matrix composites. Such high strain rates are often attributed to the presence of a very fine microstructure (with average grain size of about 0.5  $\mu\text{m}$ ) and oxide and carbide dispersions approximately 30 nm

in diameter that have an interparticle spacing of about 60 nm [418]. These particle dispersions impart stability to the microstructure. The strain-rate sensitivity exponent ( $m$ ) increases with temperature reaching values usually higher than 0.3 at the temperatures where the highest elongations are observed. Optimum superplastic elongations are often obtained at temperatures above solvus.

After introducing a threshold stress,  $n=2$  and the activation energy is equal to that corresponding to grain-boundary diffusion. These values are similar to those obtained for conventional Superplasticity and would indicate that the main deformation mechanism is grain-boundary sliding accommodated by dislocation slip. The rate-controlling mechanism would be grain-boundary diffusion [502,506,517]. Mishra *et al.* [502] claim that the small size of the precipitates allows for diffusion relaxation of the stresses at the particles by grain-boundary sliding, as illustrated in Figure 62. Higashi *et al.* [517] emphasize the importance of the presence of a small amount of liquid phase at the interfaces that contributes to stress relaxation and thus enhanced superplastic properties at temperatures above solvus. Li *et al.* [506] state that, given the small size of the particles, no load transfer

**Table 3.** Superplastic properties of some mechanically alloyed materials.

| Material   | Temperature (°C) | Strain-rate (s <sup>-1</sup> ) | Elongation (%) | Reference |
|------------|------------------|--------------------------------|----------------|-----------|
| IN9021     | 450              | 0.7                            | 300            | [511]     |
| IN90211    | 475              | 2.5                            | 505            | [512,513] |
| IN9052     | 590              | 10                             | 330            | [514]     |
| IN905XL    | 575              | 20                             | 190            | [515]     |
| SiC/IN9021 | 550              | 50                             | 1250           | [515]     |
| MA754      | 1100             | 0.1                            | 200            | [516]     |
| MA6000     | 1000             | 0.5                            | 308            | [516]     |

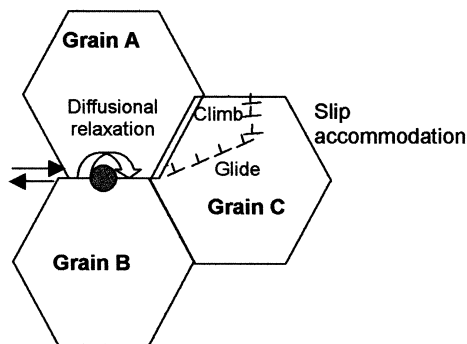


**Figure 62.** grain-boundary sliding accommodated by boundary diffusion-controlled dislocation slip.

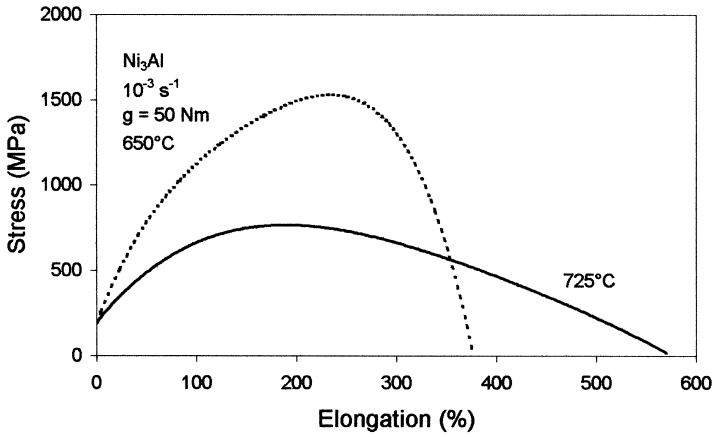
takes place and thus the values obtained for the activation energy after introducing a threshold stress are the true activation energies. According to Li *et al.*, the same mechanism (GBS rate controlled by grain-boundary diffusion) predominates during HSRS in both metal–matrix composites and mechanically alloyed materials.

## 6.6 SUPERPLASTICITY IN NANO AND SUBMICROCRYSTALLINE MATERIALS

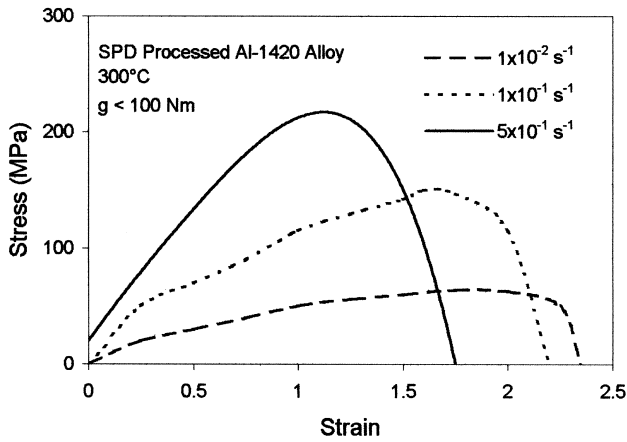
The development of grain size reduction techniques in order to produce microstructures capable of achieving Superplasticity at high strain rates and low temperatures has been the focus of significant research in recent years [480,518–522]. Some investigations on the mechanical behavior of sub-microcrystalline ( $1\ \mu\text{m} > g > 100\ \text{nm}$ ) and nanocrystalline ( $g < 100\ \text{nm}$ ) materials have shown that superplastic properties are enhanced in these materials, with respect to microcrystalline materials of the same composition [518–530]. Improved superplastic properties have been reported in metals [518–522,524–529], ceramics [523], and intermetallics [527,529,530]. The difficulties in studying Superplasticity in nanomaterials arise from (a) increasing uncertainty in grain size measurements, (b) difficulty in preparing bulk samples, (c) high flow stresses may arise, that may approach the capacity of the testing apparatus, and (d) the mechanical behavior of nanomaterials is very sensitive to the processing, due to their metastable nature.

The microscopic mechanisms responsible for Superplasticity in nanocrystalline and sub-microcrystalline materials are still not well understood. Together with superior superplastic properties, significant work hardening and flow stresses larger than those corresponding to coarser microstructures have often been observed [526–528]. Figure 63 shows the stress–strain curves corresponding to  $\text{Ni}_3\text{Al}$  deformed at  $650^\circ\text{C}$  and  $725^\circ\text{C}$  at a strain rate of  $1 \times 10^{-3}\ \text{s}^{-1}$  [Figure 63(a)] and to Al-1420 deformed at  $300^\circ\text{C}$  at  $1 \times 10^{-2}\ \text{s}^{-1}$ ,  $1 \times 10^{-1}\ \text{s}^{-1}$ , and  $5 \times 10^{-1}\ \text{s}^{-1}$  [Figure 63(b)]. It is observed in Figure 63(a) that nanocrystalline  $\text{Ni}_3\text{Al}$  deforms superplastically at temperatures which are more than  $400^\circ\text{C}$  lower than those corresponding to the microcrystalline material [532]. The peak flow stress, that reaches 1.5 GPa at  $650^\circ\text{C}$ , is the highest flow stress ever reported for  $\text{Ni}_3\text{Al}$ . Significant strain hardening can be observed. In the same way, Figure 63(b) shows that the alloy Al-1420 undergoes superplastic deformation at temperatures about  $150^\circ\text{C}$  lower than the microcrystalline material [533], and at strain-rates several orders of magnitude higher ( $1 \times 10^{-1}\ \text{s}^{-1}$  vs.  $4 \times 10^{-4}\ \text{s}^{-1}$ ). High flow stresses and considerable strain hardening are also apparent.

The origin of these anomalies is still unknown. Mishra *et al.* [528,531] attributed the presence of high flow stresses to the difficulty in slip accommodation in nanocrystalline grains. Islamgaliev *et al.* [529] support this argument. The difficulty



(a)



(b)

**Figure 63.** Stress–strain curves corresponding to (a)  $\text{Ni}_3\text{Al}$  deformed at  $650^\circ\text{C}$  (dotted line) and  $725^\circ\text{C}$  (full line) at a strain rate of  $1 \times 10^{-3} \text{ s}^{-1}$  and (b) to Al-1420 deformed at  $300^\circ\text{C}$  at  $1 \times 10^{-2} \text{ s}^{-1}$ ,  $1 \times 10^{-1} \text{ s}^{-1}$ , and  $5 \times 10^{-1} \text{ s}^{-1}$ . From Refs. [529] and [531].

of dislocation motion in nanomaterials has also been previously reported in Ref. [534]. The stress necessary to generate the dislocations responsible for dislocation accommodation is given by Ref. [528]:

$$\tau = \frac{Gb}{4\pi\lambda(1-\nu)} \left( \ln\left(\frac{\lambda_p}{b}\right) - 1.67 \right) \quad (111)$$

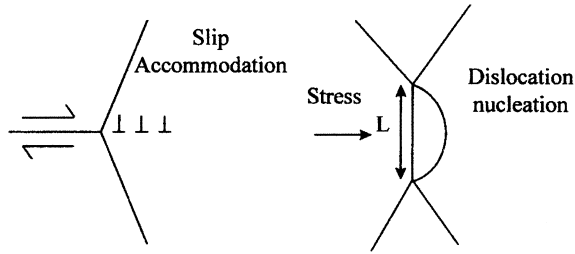


Figure 64. Generation of dislocations for slip accommodation of GBS. From Ref. [531].

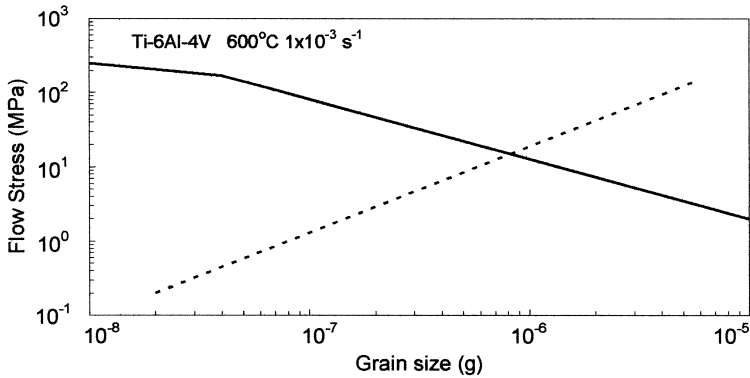


Figure 65. Theoretical stress for slip accommodation and flow stress for overall Superplasticity vs. grain size in a Ti-6Al-4V alloy deformed at  $1 \times 10^{-3} \text{ s}^{-1}$ . From Ref. [531]. (Full line: theoretical stress for slip accommodation; dashed line: predicted stress from empirical correlation  $\dot{\epsilon}_{ss} = 5 \times 10^9 (\sigma/E) 2(D_{sd}/g^2)$ ).

where  $\lambda_p$  is the distance between the pinning points and  $\tau$  is the shear stress required to generate the dislocations (see Figure 64). Figure 65 is a plot showing the variation with grain size of the stress calculated from equation (111) and the flow stress required for overall superplastic deformation [obtained from equation (100) assuming the main deformation mechanism is GBS accommodated by lattice diffusion-controlled slip]. It can be observed that, for coarser grain sizes, the flow stress is high enough to generate dislocations for the accommodation of grain-boundary sliding. For submicrocrystalline and nanocrystalline grain sizes, however, the stress required for slip accommodation is higher than the overall flow stress. This is still a rough approximation to the problem, since equation (111) does not include strain-rate dependence, temperature dependence other than the modulus, as well as the details for dislocation generation from grain boundaries. However, Mishra *et al.* use this argument to emphasize that the microcrystalline behavior can apparently



not be extrapolated to nanomaterials. Instead, there may be a transition between both kinds of behavior. The large strain hardening found during Superplasticity of nanocrystalline materials has still not been thoroughly explained.

A classification of nanomaterials according to the processing route has been made by the same authors [528,531]. Nanomaterials processed by mechanical deformation (such as ECAP) are denoted by “D” (for deformation) and nanomaterials processed by sintering of powders are denoted by “S”. In the first, a large amount of dislocations are already generated during processing, which can contribute to deformation by an “exhaustion plasticity” mechanism. Thus, the applied stress, which at the initial stage of deformation is not enough to generate new dislocations for slip accommodation, moves the previously existing dislocations. As the easy paths of grain-boundary sliding become exhausted, the flow stress increases until it is high enough to generate new dislocations. “S” nanomaterials may not be suitable for obtaining large tensile strains, due to the absence of pre-existing dislocations.

A significant amount of grain growth takes place during deformation even when Superplasticity occurs at lower temperatures. In fact, the transition from low plasticity to Superplasticity in nanomaterials is often accompanied by the onset of grain growth. This seems unavoidable, since both grain growth and grain-boundary sliding are thermally activated processes. It has been found that a reduction of the superplastic temperature is usually offset by a reduction of grain-growth temperature [527]. As the grain size decreases, the surface area of grain boundaries increases, and thus the reduction of grain-boundary energy emerges as a new driving force for grain growth. This force is much less significant for coarser grain sizes (which, in turn, render higher superplastic temperatures). Thus, the possibility of observing Superplasticity in nanomaterials, that remain nanoscale after deformation, seems small.